RSC Advances

PAPER

View Article Online
View Journal | View Issue

Cite this: *RSC Adv.*, 2015, **5**, 32643

Model peptides containing the 3-sulfanyl-norbornene amino acid, a conformationally constrained cysteine analogue effective inducer of 3_{10}-helix secondary structures†

Alessandro Ruffoni,*[a] Alessandro Contini,[a] Raffaella Soave,[b] Leonardo Lo Presti,[c] Irene Esposto,[a] Irene Maffucci,[a] Donatella Nava,[a] Sara Pellegrino,[a] Maria Luisa Gelmi[a] and Francesca Clerici*[a]

Received 4th March 2015
Accepted 27th March 2015

DOI: 10.1039/c5ra03805g

www.rsc.org/advances

The properties of the constrained tetrasubstituted 3-sulfanylnorbornene amino acid (NRB), when inserted in Ala-Aib model peptides, were extensively studied. The conformational behaviour of these models was evaluated by theoretical calculations, spectroscopic analyses and by X-ray crystallography. Taken together, our data confirm that both (*R*,*R*,*R*,*S*)- and (*S*,*S*,*S*,*R*)-NRB enantiomers possess a strong helicogenic effect when inserted in short Ala-Aib sequences, suggesting that the rigid norbornane core has a positive effect on the ability to stabilize helical secondary structures. This information will be essential for future applications in the rational design of conformationally stable peptides targeted on protein–protein interaction (PPI) surfaces.

Introduction

Protein–protein interactions (PPI) represent a central event in biological pathways and the possibility to modulate such interactions is considered of great importance.[1] Several efforts were devoted to discover new small drug-like molecules acting as modulators of PPI, but sometimes providing unsatisfactory results.[2] Recent strategies are focused on the use of *ad hoc* designed natural peptides,[3] which, however, often have a low stability, bad pharmacokinetics and an unstable conformation.[4] The exploitation of non-natural amino acids (AAs) in peptide synthesis is very useful to overcome these problems. Peptidomimetic sequences[5] are inherently resistant to proteases and peptidases and can fold into well-ordered secondary structures consisting of helices, turns and sheets.[6]

Such stabilized secondary structures might be crucial to enhance the activity and selectivity of interaction with a specific biological target. In particular, Cα-tetrasubstituted α-amino acids (CTAAs) were used to stabilize bioactive helical peptides.[7]

In our laboratory, synthetic procedures for the preparation of several constrained CTAAs[6b,8–11] were developed. Some of these were successfully used for the preparation of short peptides, which fold into stable helical structures. Clearly, the ability of a new amino acid to induce a defined secondary structure must be proved by experimental data. Moreover, the stereochemistry of the new AA is of fundamental importance: depending on the enantiomer chosen, a different conformational stability of the resulting isomeric peptide could be expected.[6b]

In the last few years interest toward Rac1 protein, whose activation is mediated by Tiam1, has increased for its role in cancer and cardiovascular diseases.[12] In a recent article we described the design and synthesis of a new class of small molecules acting as Rac1-Tiam1 PPI inhibitors.[13] These compounds, even if of great interest, showed, as other inhibitors reported so far, a potency too low for a potential use in therapy (low μM range).[14]

Preliminary studies performed in our laboratory identified a peptide sequence containing hot and warm spots in the 13 residue long helix of Tiam1, CR3 (I1187-L1199); however, this portion cannot be used as a stand-alone peptide inhibitor, since it is predicted to be disordered.[15] Taking into account the above considerations, the introduction into the peptide sequence of one or more CTAAs would result in a helical structured more stable peptide. According to recent studies of our group,[16] we chose the 3-benzylsulfanyl amino ester **1** containing the norbornene amino acid (NRB) as a CTAA. First of all we planned the

[a]*Università degli Studi di Milano, Dipartimento di Scienze Farmaceutiche, Sezione di Chimica Generale e Organica "Alessandro Marchesini", Via Venezian 21, 20133 Milano, Italy. E-mail: alessandro.ruffoni@unimi.it; francesca.clerici@unimi.it; Fax: +390250314476; Tel: +390250314472*

[b]*CNR-Istituto di Scienze e Tecnologie Molecolari, Via Golgi 19, 20133 Milano, Italy*

[c]*Università degli Studi di Milano, Dipartimento di Chimica, Via Golgi 19, 20133 Milano, Italy*

† Electronic supplementary information (ESI) available: Experimental protocols for the synthesis of peptides **2a** and **2b** ^{1}H and ^{13}C spectra for all compounds and crystallographic data in CIF. CCDC 989313 and 989314. For ESI and crystallographic data in CIF or other electronic format see DOI: 10.1039/c5ra03805g

preparation of model pentapeptides Ac-Ala-NRB-Ala-Aib-Ala-NH_2 of general formula 2 (Fig. 1) by using both enantiomers of NRB. The conformational behavior of these models and the ability of the two different enantiomers of NRB to induce a defined secondary structure was evaluated by theoretical calculation, spectroscopic analyses, and by X-ray crystallography. These information, besides being of importance for developing new peptidomimetic inhibitors of Rac1-Tiam1 PPI, might lay the ground for future applications in the rational design of other new bioactive peptidomimetics.

Results and discussion

The synthesis of **1** (R = Et) previously described by us,[10] was scaled up to 1.5 grams in order to assure the availability of a congruous amount of starting NRB.

For the preparation of pentapeptides **2** several strategies were tested.

Firstly, we planned to use the procedure depicted in Scheme 1, whose key step consists in coupling the diastereoisomeric dipeptides Ac-Ala-NRB-OH (**3**) with the TFA salt of the tripeptide H-Ala-Aib-Ala-NH_2 (**4**), synthesized by solid phase synthesis.[6b]

Accordingly, **1** was submitted to hydrolysis obtaining the fast conversion of the ester into acid in high yield but, as already observed in similar cases,[10] together with the addition of HCl to the double bond. Operating in basic condition resulted in very slow reaction, low yield and purification difficulties. To overcome this problem the double bond of **1** was reduced providing **5** (Scheme 2), which was reacted with FmocAlaF as both reagent and resolving agent.[17] Unfortunately, an inseparable mixture of the two expected diastereoisomers was obtained. Fmoc deprotection (piperidine, DMF) afforded the two diastereoisomers **6a** and **6b** (95% overall yield), which were partially separated by simple flash chromatography.

The two compounds were analysed to ascertain their correct structure, but very little differences were observed in protons chemical shifts (^{1}H NMR, see Experimental), the main

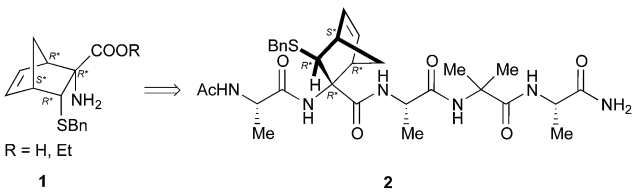

Fig. 1 Pentapeptides from norbornene amino acid precursor.

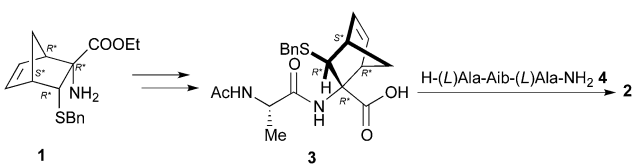

Scheme 1 Original synthetic plan.

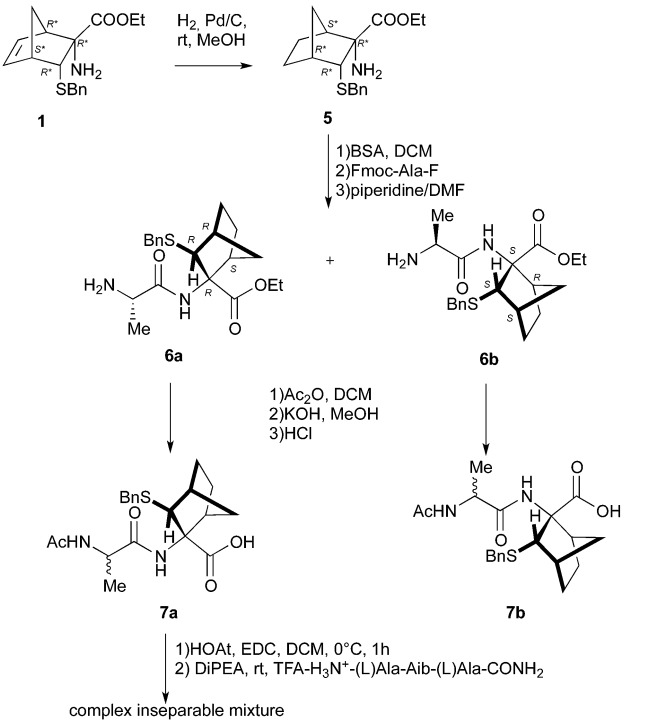

Scheme 2 Synthesis of pentapeptides: first synthetic approach.

difference being the methylenic protons of ester function (see ESI†). A confirmation of the correct structure and stereochemistry came from X-ray analyses. Suitable crystals were obtained only for one of the two diastereoisomers (**6a**: AcOEt : $CHCl_3$ 1 : 1; RT; 24 h). Finally, acetylation of **6a** and **6b** followed by hydrolysis of the ethyl esters provided **7a** and **7b**. Unfortunately, the hydrolysis led to racemization of the alanine stereocenter or to a partial cleavage of amides bond despite to numerous reaction conditions tested (NaOH, KOH, LiOH, or HCl 3 N, 6 N, 37%). However, we tried to couple the crude containing **7a** with the tripeptide H-Ala-Aib-Ala-NH_2 (**4**) operating in standard conditions (EDC 1.1 eq., HOAt 1.1 eq., DCM, 0 °C), but we obtained an inseparable mixture.

The main drawbacks of the synthetic way described above were the limited scalability of the known solid phase synthesis of the tripeptide H-Ala-Aib-Ala-NH_2 (**4**)[6b] and the racemization events during the hydrolytic procedures. Consequently, first of all we set up a linear Boc chemistry solution strategy that allowed us to prepare the tripeptide **4** as a free amine in 50% overall yield on a gram scale (Scheme 3). The process consisted in the coupling between H-Ala-NH_2 (**9**) or the dipeptide H-Aib-Ala-NH_2 (**11**) with the Boc-protected AA **8** and, respectively, **12** in standard conditions (see Scheme 3). The coupling afforded respectively the dipeptide Boc-Aib-Ala-NH_2 (**10**) and the tripeptide Boc-Ala-Aib-Ala-NH_2 (**13**).

The Boc deprotection of **10** was, as usual, realized by treatment with TFA/DCM. On the other hand the deprotection of **13**, affording the desired compound **4**, was obtained by microwave (20 + 20 min, 150 °C) mediated thermal decomposition of Boc protection.[18]

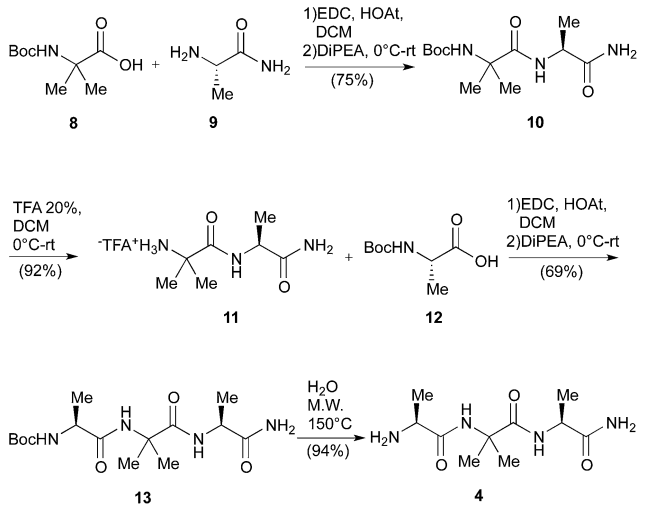

Scheme 3 Gram scale synthesis of the tripeptide **4**.

In such way we avoided the formation of the corresponding TFA salt, negatively affecting the key coupling with the Boc protected NRB **15**.

Having in hand a good protocol for the preparation of compound **4**, we reconsidered the use of AA **1** and a different strategy was set up to obtain peptides **2**.

First, the Boc-protected NRB **15** was prepared in good yield on gram scale according to standard protocols through the reaction of **1** with Boc anhydride, giving **14**, followed by hydrolysis of the ester function in basic conditions (KOH 3 M in MeOH, Scheme 4). Compound **15** was coupled with the tripeptide **4** in the conditions reported in Scheme 4, affording the two expected diastereoisomeric tetrapeptides **16a** and **16b** (yield 75%) that were successfully separated by flash chromatography. The following microwave assisted Boc deprotection afforded compounds **17a** (82%) and **17b** (88%) without racemization.

Peptides **17a** and **17b** were then reacted with Ac-Ala-OH in different conditions (Scheme 5). To optimize the yields and to minimize racemization, several synthetic protocols were tested which are reported, together with yields and percentage of racemization, in Table 1, starting from **17a** (entries 1–5) and **17b** (entries 6–10), respectively. The best conditions to obtain compound **2a** from **17a** resulted in using classic coupling condensation conditions (HOAt 1.1 eq., EDC 1.1 eq., DIPEA 2.2 eq., DCM, entry 1). In this way, pure compound **2a** was obtained after HPLC purification (40%).

In the case of **17b** partially satisfactory results were obtained by using EEDQ (entry 7) as the condensing agent in THF as the solvent. Racemization process was avoided but the yield was still low.

It is well known that MWs are able to promote unfolding of peptides and this effect is exploited in solid phase peptide synthesizers, thus allowing a general increase of yields. Nevertheless, to our knowledge, few examples are present in the literature concerning the use of MW in solution peptide synthesis,[19] and only one example employing an unnatural AA (Aib).[20] As a result, a sample containing **17b**, Ac-Ala-OH and EEDQ in THF was irradiated for 30′ at the lowest temperature reachable by a conventional compressed air-cooled MW reactor

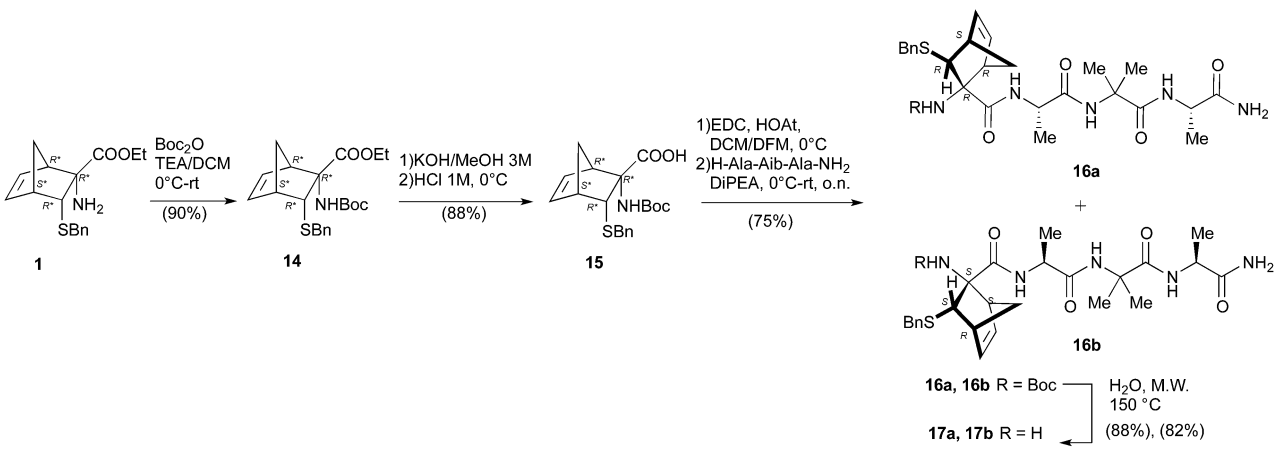

Scheme 4 Synthesis of peptides **17a** and **17b**.

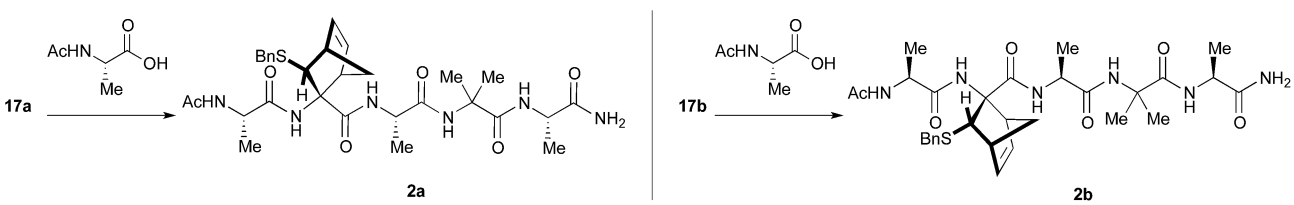

Scheme 5 Synthesis of projected peptide **2a** and **2b**.

Table 1 Reaction conditions for the synthesis of **2a** and **2b**

Entry	Reagent	Solvent	Reaction conditions	T (°C)	Yield (%)	Racemization (%)
1	**17a**	DCM	HOAt, EDC, DIPEA	0–rt	40	5
2	**17a**	THF	EEDQ, MW (70 Watt), air cooling, 30 min	60–70 °C	60	20
3	**17a**	DCM	HOBt, EDC, DIPEA	0–rt	5	—
4	**17a**	DCM	HBTU, EDC	0–rt	—	—
5	**17a**	DCM	HBTU, DIPEA	0–rt	10	—
6	**17b**	THF	EEDQ MW (70 Watt), air cooling, 30 min	60–70	60	0
7	**17b**	THF	EEDQ	0–rt	35	0
8	**17b**	DCM	HOAt, EDC, DIPEA	0–rt	30	15
9	**17b**	DCM	HOAt, EDC, DIPEA	0–rt	—	—
10	**17b**	DCM	HBTU, DIPEA	0–rt	Complex mixture	—

(80 Watt) (Table 1, entry 6). After 30 minutes, the solution was by cooled and peptide **2b** directly precipitated in pure form in 60% yield.

Conformational study

X-ray diffraction

Single crystals of **6a** were grown by slow evaporation from a mixture 1 : 1 of ethyl acetoacetate and chloroform, while those of compound **2b** by slow evaporation from a solution of acetonitrile (ESI†).

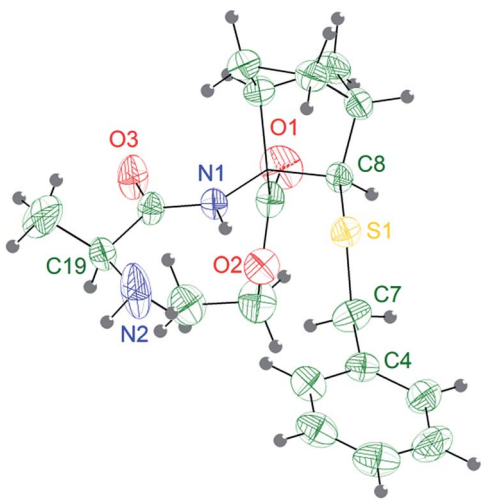

Fig. 2 Stereoview of the molecular structure of compound **6a** at 298 K, showing 30% probability displacement ellipsoids.

X-ray analysis of 6a. The analysis allowed the determination of the absolute stereochemistry of the five asymmetric carbons (Fig. 2) and evidenced hydrogen bonding interactions (ESI pp. S56†).

The Ala group undergoes a significant apparent thermal motion, which could imply some kind of disorder. As for the crystal packing (ESI pp. S56†), the system forms *zig-zag* ribbons of head-to-tail hydrogen bonded (HB) molecules parallel to the *a* axis. The only relevant HB contact involves one H atom belonging to the terminal amine group and the amidic oxygen of an opposing Ala unit. Another possible HB donor is the amidic N–H group, which is actually involved in an intramolecular short contact with the sulfur atom (Fig. 2 and Table 2).

X-Ray analyses of 2b. The analysis confirmed the absolute stereochemistry of NRB and that no racemization occurred during the whole synthetic process. Interestingly, the asymmetric unit is composed of two molecules (**2b**^{i} and **2b**^{ii} hereinafter) as shown in Fig. 3a and b. The φ and ψ dihedrals of both the conformations present in the crystal cell were close to the ideal values of a 3_{10}-helix ($\varphi = -49$; $\psi = -26$) with a right handed screw sense, as shown in Table 3.

Four consecutive intramolecular short contacts occur in both conformers. They involve the NH protons of $CONH_2$, Ala(5)NH, Aib(4)NH and Ala(3)NH, as listed together with their geometrical parameters in Table 4. Three of them are common in the two conformers, *i.e.* they involve the same NH groups as donors (N1, N2 and N4) and the same O atoms as acceptors (O5, O3 and O1). Again in both the conformers, out of the two NH protons of the $CONH_2$ group, only one is involved in a short intramolecular contact: while in conformer **2b**^{i} the interaction arises between the N6A–HN6A2 group and atom O1A, in **2b**^{ii} it involves the N6B–HN6B2 and atom O2B. The

Table 2 Relevant short H···O,S contacts in **6a**. Values are given in Å and degrees, with sensible estimated standard deviations reported in parentheses

D–H···A	D–H	Distance H···A	Distance D···A	Angle D–H···A	Symmetry[a]
N2–H2B···O2	0.90	2.18	2.990(4)	149.3	$-1/2 + x$, $1/2 - y$, $1 - z$
N1–HN1···S1	0.86	2.48	2.995(2)	119.0	x, y, z[b]

[a] Symmetry operation generating the acceptor ('A') atom. [b] Intramolecular contact.

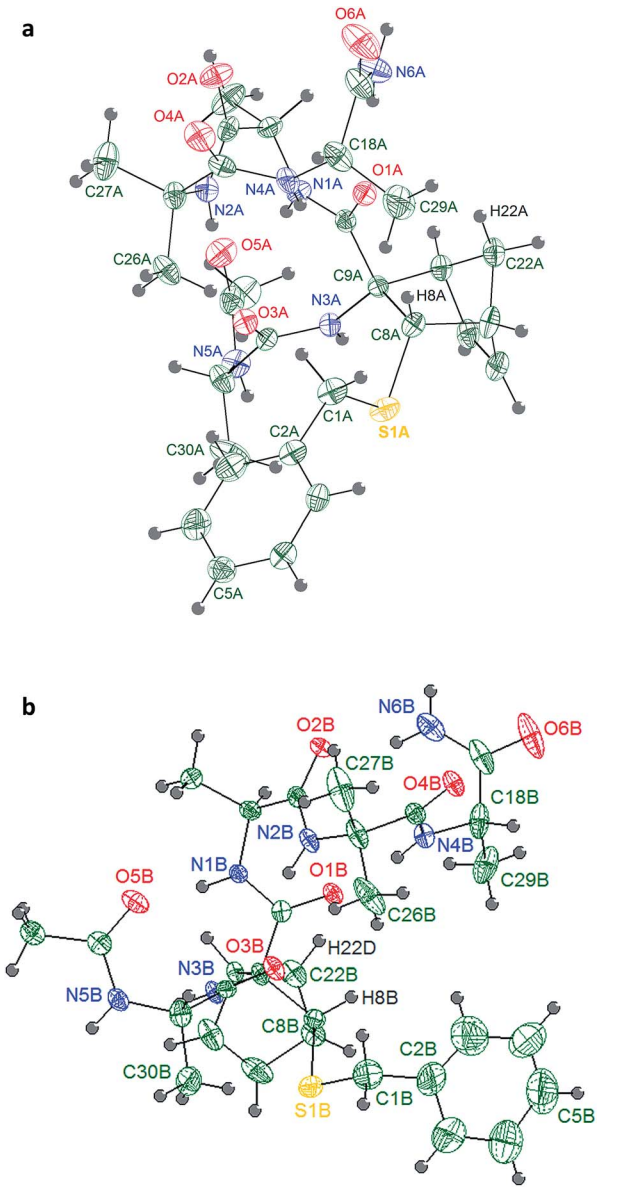

Fig. 3 (a) Stereoview of the molecular structure of compound **2b** in the crystal state at 150 K, showing 50% probability displacement ellipsoids. Only the molecule numbered as **2b**^{i} in the asymmetric unit is shown. (b) Stereoview of the molecular structure of compound **2b** in the crystal state at 150 K, showing 50% probability displacement ellipsoids. Only the molecule numbered as **2b**^{ii} in the asymmetric unit is shown.

pattern of H bonds underlined by the crystal structure completely reflects the typical distribution i–i + 3 of 3_{10}-helix for the conformer **2b**^{ii}. Regarding **2b**^{i} the 3_{10}-helix H bond distribution is respected except for the $CONH_2$ proton that present a i–i + 4 hydrogen bond interaction typical of α-helix. Such deviation of **2b**^{i} from ideal values for the terminal Ala(5) is also detectable in the angles ψ_4 and φ_4 that differ much more from ideal 3_{10}-helix than in **2b**^{ii}.

Weak hydrogen interactions (*i.e.* C–H···O, C–H···N and C–H···π)[22] have been found to be critical in stabilizing different molecular geometries.[23–28] In a previous work, our computational model underlined that the formation of an intra-residue C–H···O hydrogen bond was responsible of the helix stabilization exerted by an unsubstituted norbornene AA included in the same peptide model herein described.[16] In both **2b**^{i} and **2b**^{ii}, it can be noticed the presence of a C–H···O interaction between H22A and O1A, corresponding to that observed in the computational analysis of the unsubstituted norbornene, but also an additional interaction between H8A and O1A (Table 4), which might further enhance the NRB helix stabilizing power thanks to the correct orientation of ψ_2.

Table 3 Dihedral angle simulated and observed in the crystal structure[a]

	Simulated[b]	Peptide **2b**^{i}	Peptide **2b**^{ii}
ψ_0		−57.4	−54.4
ψ_1	−13.61 ± 34.74	−32.8	−42.0
φ_1	−53.12 ± 16.48	−50.0	−53.5
ψ_2	−29.37 ± 14.99	−32.1	−39.9
φ_2	−62.45 ± 18.99	−65.3	−63.1
ψ_3	−26.30 ± 15.16	−17.2	−17.9
φ_3	−55.06 ± 9.96	−55.5	−50.4
ψ_4	−24.25 ± 12.81	−42.2	−34.8
φ_4	−106.84 ± 35.15	−81.6	−73.8
φ_5		−48.1	−20.3

[a] **2b**^{i} and **2b**^{ii} are the two different conformers of peptide **2b** in the crystal cell. [b] Dihedral values obtained by REMD simulation, as described in the computational analysis section.

Moreover, to our knowledge, only few example of crystal structures of pentapeptides containing both proteogenic and non proteogenic AAs have been reported so far containing at least two non proteogenic AAs.[21] The obtainment of a well-defined crystal structure for a pentapeptide containing only two non-proteogenic AAs, Aib and NRB, suggests that the pentapeptide is strongly structured.

NMR spectroscopy

Both peptides **2a** and **2b** were subjected to NMR conformational analysis. Experiments were performed in both cases in CD_3CN (20 mM) in order to avoid the hydrophobic collapse typical of chlorinated solvent and simulate as much as possible a polar medium. Homonuclear and heteronuclear 2D NMR experiments permitted an overall assignment of **2a** and **2b** proton and carbon resonances (see ESI, pp. S4–S12,† COSY, HSQC, HMBC spectra).

NOESY experiments on compound 2b. NOESY spectra allowed the identification of all sequential short range NH_i–NH_{i+1} cross peaks in the amide region (ESI, pg. S8†), that are diagnostic of helical conformation.[29]

The analysis of $C^{\alpha(\beta)}H$–NH enabled the discrimination between the 3_{10}-helix and the α-helix structures. No $C^{\alpha}H_i$–NH_{i+4} cross-peaks inherent of α-helix were detectable in the NOESY spectra, but many diagnostic $C^{\alpha}H_i$–NH_{i+3} and $C^{\alpha}H_i$–NH_{i+2} medium range cross-peak signals typical of 3_{10}-helix were present. An inspection of the fingerprint area of NOESY spectrum revealed three $C^{\alpha}H_i$–NH_{i+3} [Ala(1)H^{α}–Aib(4) NH, Ala(3)H^{α}–$CONH_2$ (Fig. 4) and AcMe–Ala(3)NH, (Fig. 5)], and

Table 4 Intramolecular H-bond parameters observed for compound **2b** in the crystal state. Estimated standard deviations are reported in parentheses. Distances in Å angles in (°)

Conformer	Group	Donor D–H	Acceptor A	Distance D···A	Distance H···A	Angle D–H···A
2b^{i}	Ala(3)	N1A–HN1A	O5A	2.939(4)	2.116(3)	159.8(2)
2b^{ii}		N1B–HN1B	O5B	3.003(4)	2.277(3)	142.2(2)
2b^{i}	Aib(4)	N2A–HN2A	O3A	2.960(3)	2.134(2)	160.9(2)
2b^{ii}		N2B–HN2B	O3B	2.983(4)	2.176(2)	156.0(2)
2b^{i}	Ala(5)	N4A–HN4A	O1A	2.984(4)	2.284(3)	138.6(2)
2b^{ii}		N4B–HN4B	O1B	3.032(4)	2.206(2)	160.9(2)
2b^{i}	$CONH_2$	N6A–HN6A2	O1A	3.141(4)	2.288(2)	171.8(2)
2b^{ii}		N6B–HN6B2	O2B	2.910(4)	2.122(3)	151.9(2)
2b^{i}	NRB(2)	C8A–H8A	O1A	2.796(4)	2.274(3)	112.3(2)
2b^{ii}		C8B–H8B	O1B	2.851(4)	2.365(3)	109.9(2)
2b^{i}	NRB(2)	C22A–H22A	O1A	3.131(4)	2.453(4)	126.6(2)
2b^{ii}		C22B–H22D	O1B	3.154(4)	2.480(3)	126.4(2)

two $C^{\alpha}H_i$–NH_{i+2} [Ala(1)H$^{\alpha}$–Ala(3)NH (Fig. 4), AcMe–NRB(2)NH (Fig. 5)] supporting the hypothesis of a 3_{10}-helix structure.

Also medium and short range signals $C^{\beta}H_i$–NH_{i+3} (Ala(1)-Me–Aib(4)NH, Ala(3)Me–$CONH_2$ and Aib(4)Me–Ala(1)NH, Fig. 6) and $C^{\beta}H_i$–NH_{i+2} [Ala(5)Me–Ala(3)NH, Aib(4)Me–$CONH_2$ (Fig. 5) and NRB(2)H3–Aib(4)NH (Fig. 4)] confirmed the initial hypothesis.

Finally, a high degree of structuration of peptide **2b** could be inferred by the presence of an unusual and intense long range cross-peak between the H3 proton of the norbornene scaffold and the Me groups of Ala(5) and Ala(1)α–Aib(4)Me as shown in Fig. 6.

NOESY experiments on compound 2a. Despite the overlap of two H$^{\alpha}$ and two NH amide protons which complicated the interpretation of NMR data, valuable structural information were obtained. Using standard sample conditions in CD_3CN (20 mM) all sequential short range NH_i–NH_{i+1} interactions were visible (ESI, pg. S13†) except the interaction between Ala(5)NH–$CONH_2$, obscured by the phase of diagonal peaks. By acquiring the NOESY spectrum at lower concentration (8 mM), we identified the entire sequence confirming an helical construct for **2a** (ESI, pg. S13†).[23]

Moreover, 3D structural information present in the $C^{\alpha(\beta)}$H–NH region of the NOESY spectrum of **2a** were enough to confirm the

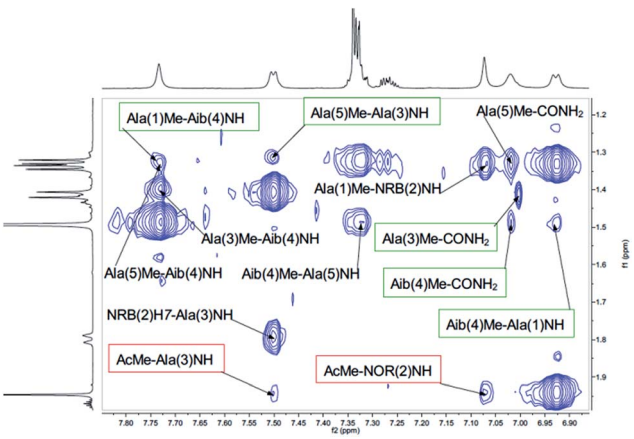

Fig. 5 C^{β}H–NH cross peaks in the NOESY spectrum (τ_m 500 ms, BBI probe, 300 K, 500 MHz) of peptide **2b** in CD_3CN (20 mM). Medium range $C^{\beta}H_i$–NH_{i+3} and $C^{\beta}H_i$–NH_{i+2} diagnostic for helical structure (α red box, β green box).

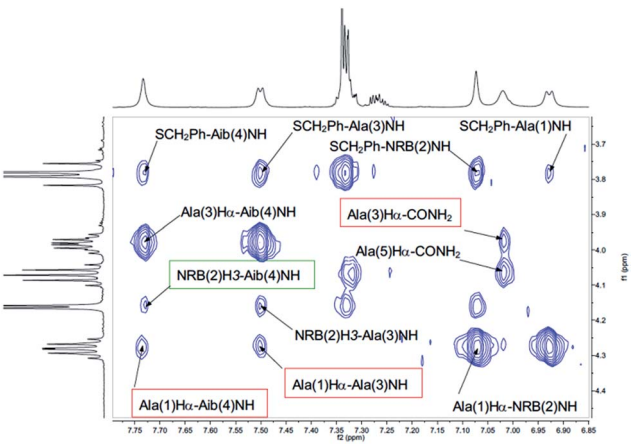

Fig. 4 C^{α}H–NH cross peaks in the NOESY spectrum (τ_m 500 ms, BBI probe, 300 K, 500 MHz) of peptide **2b** in CD_3CN (20 mM). Sequential short range $C^{\alpha}H_i$–NH_{i+1} signals diagnostic for structured peptide. Medium range $C^{\alpha}H_i$–NH_{i+3} and $C^{\alpha}H_i$–NH_{i+2} signals typical of 3_{10}-helix (α red box, β green box).

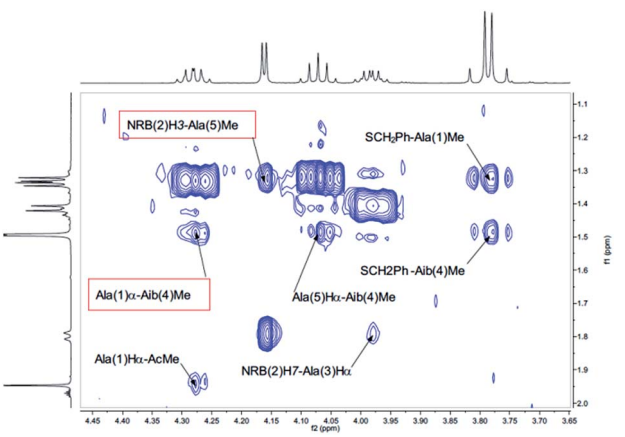

Fig. 6 $^{\alpha}$H–Me of the NOESY spectrum (τ_m 5000 ms, BBI probe, 300 K, 500 MHz) of peptide **2b** in CD_3CN (20 mM).

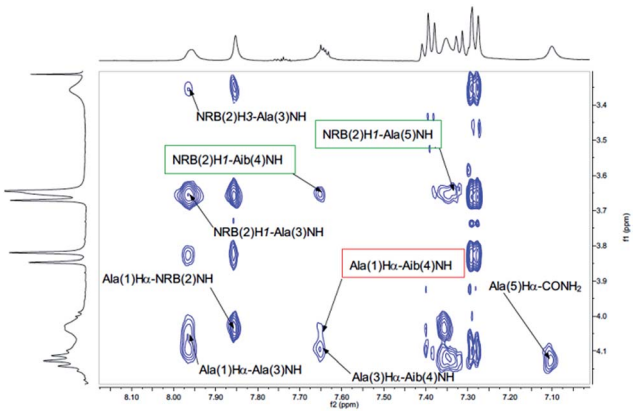

Fig. 7 $C^{\alpha}H$–NH cross peaks in the NOESY spectrum (τ_m 500 ms, BBI probe, 300 K, 500 MHz) of peptide **2a** in CD_3CN (20 mM). Sequential short range $C^{\alpha}H_i$–NH_{i+1} signals diagnostic for structured peptide. Medium range $C^{\alpha(\beta)}H_i$–NH_{i+3} and $C^{\alpha(\beta)}H_i$–NH_{i+2} signals typical of 3_{10}-helix (α red box, β green box).

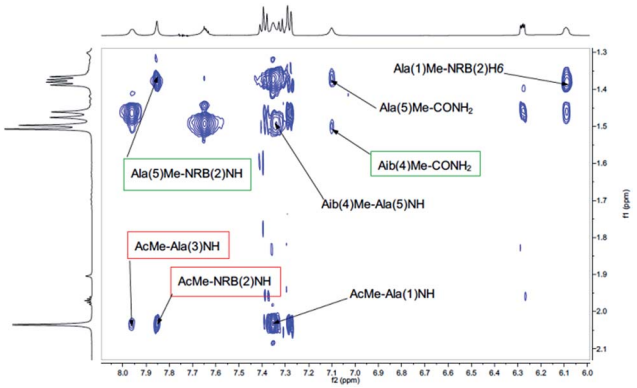

Fig. 8 $C^{\beta}H$–NH of the NOESY spectrum (τ_m 500 ms, BBI probe, 300 K, 500 MHz) of peptide **2a** in CD_3CN (20 mM). Sequential short range $C^{\alpha}H_i$–NH_{i+1} signals diagnostic for structured peptide. Medium range $C^{\alpha(\beta)}H_i$–NH_{i+3} and $C^{\alpha(\beta)}H_i$–NH_{i+2} signals typical of 3_{10}-helix (α red box, β green box).

preference of a 3_{10}-helix over a α-helix. Detectable interactions $C^{\alpha(\beta)}H_i$–NH_{i+2} (Ala(1)H^{α}–Ala(3)NH, NRB(2)H^{β}–Aib(4)NH, AibMe–$CONH_2$ and AcMe–NRB(2)NH) and $C^{\alpha}H_i$–NH_{i+3} (Ala(1)H^{α}–Aib(4)NH, NRB(2)H^{β}–Ala(5)NH and AcMe–Ala(3)NH) are shown in Fig. 7 and 8. In conclusion, the absence of $C^{\alpha(\beta)}H_i$–NH_{i+4} cross peaks in the NOE spectrum suggests that both enantiomers of **1**, once inserted in the model peptides **2a** and **2b**, stabilize a 3_{10}-helical structure.

VT-NMR and DMSO$_{d6}$ titration. To confirm the presence of a 3_{10}-helical structure, the H-bond network within the peptide backbone was analyzed by measuring the temperature coefficient of the chemical shifts ($\Delta\delta$(NH)/ΔT) for each NH of **2a** and **2b**, as well as the variation of chemical shift by DMSO-d_6 titration ($\Delta\delta$/ΔDMSO-d_6 v/v).

Three stable consecutive H-bonds, involving NH protons of $CONH_2$, Ala(5)NH and Aib(4)NH, are detected (Fig. 9 and 10) demonstrating, according to our proposal, a full helical construct for both peptides **2a** and **2b**. In peptide **2b**, Ala(3) NH also presents very low $\Delta\delta$ values, supporting the presence of a further intramolecular H-bond which is only compatible with 3_{10}-helical structure. Indeed, the N terminal Ala(1)NH coefficient and, as might be expected, one NH proton of $CONH_2$ group are near to the limit of −4.5 ppb K^{-1} that points out the not H-bonded NH protons. The DMSO-d_6 titration reflects the result of VT-NMR, since no variation of chemical shift are detectable for one NH proton of $CONH_2$ group, Ala(5)NH, Aib(4)NH and Ala(3)NH endorsing the presence of four H-bonds typical of 3_{10}-helix (Fig. 10). In both experiments related to **2a** and **2b**, the NRB(2)NH amide proton showed an unexpected stability. Considering that NH solvent exposition influences, to varying degrees, both the variable-temperature analysis and DMSO-d_6 titration, such result could be a false positive ascribed to the solvent exclusion sphere generated by the norbornene scaffold and the benzylsulfanyl group, as supported by NOESY spectra. The same hypothesis could also explain the high $\Delta\delta$ observed for Ala(3)NH in **2a**, which disagrees with the extremely stable trend found in DMSO-d_6 titration.

Non-magnetic equivalence. Lastly, a proof of an high content of a preferred helical conformation could be deduced from the anisochronicity of the ^{13}C NMR signals of the diastereotopic methyl groups in Aib(4). Considering that neighboring chiral residues could not induce a non-magnetic equivalence (NME) higher than 0.5 ppm, the large NME with value of 3.07 ppm (26.26–23.19 ppm, ESI, pg. S14†) for peptide **2b** and 3.88 ppm (26.60–22.72 ppm, ESI, pg. S15†) for peptide **2a** could only derive from the presence of a stable helical secondary structure.[30]

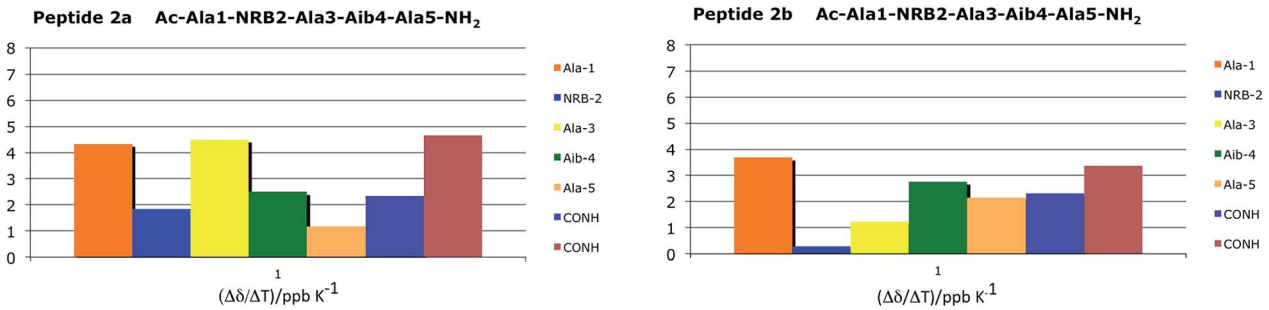

Fig. 9 Temperature coefficients for amide protons chemical shifts of **2a** and **2b** (CD_3CN 10 mM) in a range temperature of 273–335 K.

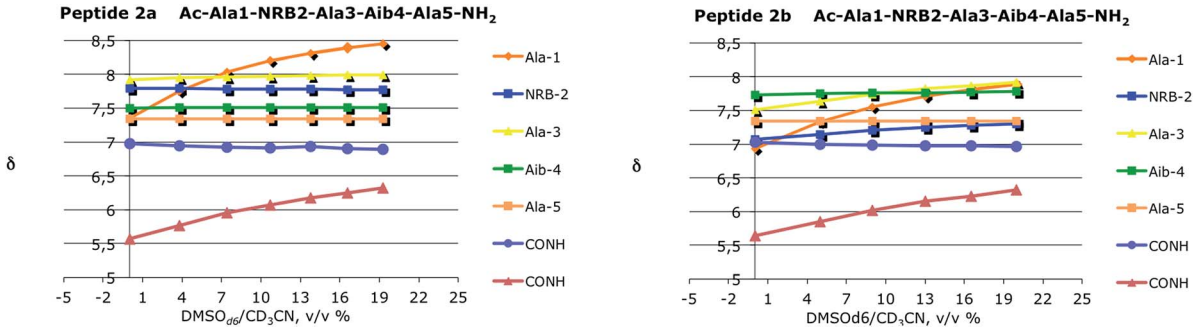

Fig. 10 Chemical shift variation for amide proton in function of DMSO-d_6 v/v% of **2a** and **2b** (CD_3CN 10 mM) in a range of 0–22 v/v%.

Computational analysis

In order to gain a deeper knowledge about the folding preferences of peptides **2a** and **2b**, based on the two enantiomers (*R*,*R*,*R*,*S*) and (*S*,*S*,*S*,*R*)-NRB, we planned a molecular dynamics (MD) study of the two pentapeptides models using the Amber12 package.[31] The replica exchange molecular dynamics (REMD) method,[32] a generalized-ensemble algorithm performing random walks in energy space, thus helping a system to escape from local energy traps, has been successfully adopted in secondary structure predictions due to its improved sampling capabilities over standard MD runs. REMD simulations (12 replicas with temperatures exponentially spaced between 260 and 660 K) were then performed by starting from extended conformations and by using a protocol previously optimized for similar questions.[6b] The peptide was simulated for 50 ns, and analyses were performed on the final 25 ns of the 308.5 K trajectory, being this temperature the closest one to experimental conditions. Trajectories were analyzed in terms of H-bonds, secondary structure and cluster analyses (Tables 5–7). Although the adopted simulation protocol already proved to be successful in predicting the structure of similar peptide models containing CTAAs,[6b] the comparison of the representative structure obtained from a cluster analysis of the REMD trajectory of peptide **2b** with the corresponding crystal structure further supported the reliability of the method adopted here (Fig. 11 and Table 3).

As we can see from H-bond analysis (Table 5), both peptides **2a** and **2b** are characterized by two $i+3 \rightarrow i$ H-bonds, which are typical of 3_{10}-helices, between residues 1–4 (Ala(1) and Aib(4), respectively) and 2–5 (NRB(2) and Ala(5), respectively). Although the overall H-bond occupancy in **2a** and **2b** is comparable, it can be observed that the most stable H-bond is found between Ala(1) and Aib(4) (occupancy = 68.4%) in **2a**, while in **2b** it is between NRB(2) and Ala(5). In both structures, the third observed H-bond is of the $i+4 \rightarrow i$ type, indicative of an α-helix, and has an occupancy of 2.5 and 1.6%, respectively, suggesting that this secondary structure is only occasionally sampled.

The secondary structure analysis (Table 6), based on the DSSP method,[33] while confirming the results of H-bond analysis, provided per-residue information on the secondary structure. Interestingly, as also observed from the H-bond analysis, (*R*,*R*,*R*,*S*)-NRB seems to propagate the 3_{10}-helix stabilization toward the N-terminus, while the (*S*,*S*,*S*,*R*)-NRB enantiomer seems to exert its stabilizing effect mostly toward the C-terminus of the model peptide.

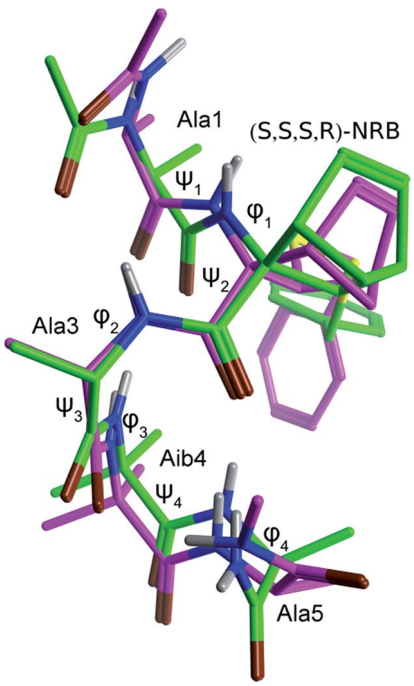

Fig. 11 Comparison between the X-ray structure of **2b** (carbon colored in green) and the representative geometry of the most populated cluster coming from the cluster analysis of the 308.5 K REMD trajectory of **2b** (RMSD (Cα) = 1.1 Å).

Table 5 H-bond[a] analysis of the last 25 ns of the 308.5 K ff99SB REMD trajectory for peptides **2a** and **2b**

	2a (*R*,*R*,*R*,*S*)-NRB	**2b** (*S*,*S*,*S*,*R*)-NRB
H-bonds	Occupancy	
Ala(1) C=O···HN Aib(4)	68.4%	46.4%
Ala(1) C=O···HN Ala(5)	2.5%	1.6%
NRB(2) C=O···HN Ala(5)	54.2%	73.4%

[a] Only H-bonds with an occupancy >1% are reported. H-bonds involving the capping Ac and NHMe groups are not reported.

Further confirmation came from the cluster analysis of the REMD trajectories. As reported in Table 7, the first three most populated cluster represent over the 95% of the total population for both **2a** and **2b** peptides. Concerning **2a**, φ and ψ values for the representative structure of cluster #1 (pop. = 79.1%) fall within the helix region, with a quite significant deviation only for the φ_4 dihedral angle of the C-terminal Ala(5). A quite wide ψ_2 dihedral angle is also observed (−57.7 deg.), possibly due to the steric hindrance between the –SBn group of NRB(2) and the $-CH_3$ of Ala(3) (C3′HH–CH_2– distance = 2.5 Å); (see figure reported in the ESI, pg S52†) cluster #2, which is significantly populated (pop. = 20.3%), corresponds to a partially folded structure where φ and ψ values for residues 1–3 fit with a right-handed helix, while Aib(4) φ and ψ dihedrals angles fall in the left-handed helix region, analogously to what observed for other CTAAs.[6b,16] Clusters #3–5 are barely populated (pop. = 0.3, 0.3 and 0.0%, respectively) and their representative structures correspond to unordered conformations. Concerning peptide **2b**, cluster #1 (pop. = 82.6%) also corresponds to a well ordered 3_{10}-helix and, differently from what observed for **2a**, the ψ_2 dihedral angles also fits with such a secondary structure. Indeed, due to the opposite stereochemical configuration, the –SBn group of NRB(2) points away from the helix core (Fig. S8 and pg S53, ESI†). Cluster #2, 8.7% of the total population, represents a folding intermediate with most of the φ and ψ dihedral angles falling in the left-handed helix region, while, interestingly, the representative structure of cluster #3 (pop. = 6.0%), corresponds to a completely folded left-handed helix (Fig. S6, page S55 ESI†), a secondary structure not observed for **2a** (figure reported in the ESI, pg S52†). Clusters #4 and #5, overall representing 2.7% of the total population, correspond to an unfolded conformation and a left-handed folding intermediate, respectively. Taken together, in agreement with the experimental result, the above data confirm that both (*R*,*R*,*R*,*S*)- and (*S*,*S*,*S*,*R*)-NRB enantiomers possess a strong helicogenic effect when inserted in short Ala-Aib sequences. In our previous work on the Azn CTAA[6b] only the (*R*)-enantiomer was shown to be helicogenic within Ala-Aib pentapeptides, suggesting that the rigid norbornane core plays a positive effect on the ability to induce helical secondary structures. However, considering the results from REMD simulations and cluster analyses, it cannot be excluded that the (*S*,*S*,*S*,*R*)-NRB enantiomer could also behave as a powerful inducer of left-handed helices if coupled with D-AAs and/or achiral CTAAs such as Aib.

Table 6 Secondary structure analysis[a] of the last 25 ns of the 308.5 K ff99SB REMD trajectory for peptides **2a** and **2b**

	2a (*R*,*R*,*R*,*S*)-NRB			**2b** (*S*,*S*,*S*,*R*)-NRB		
	3_{10}-helix	α-helix	Turn	3_{10}-helix	α-helix	Turn
Ala(1)	67.2	5.8	12.3	32.3	1.8	9.6
NRB(2)	79.7	6.1	13.2	47.3	1.9	10.8
Ala(3)	82.5	6.1	10.7	71.1	1.9	18.6
Aib(4)	66.2	6.4	24.6	67.8	2.0	25.4
Ala(5)	44.1	1.3	31.4	52.6	0.4	31.4

[a] Values are reported as a percentage of the total. The difference to 100% is the percentage of unordered secondary structure.

Table 7 Geometrical parameters for the most representative structures deriving from the cluster analysis[a] of the final 25 ns of the 308.5 K ff99SB REMD trajectory for peptides **2a** and **2b**. Cluster populations (%) are reported in parenthesis

	2a (*R*,*R*,*R*,*S*)-NRB		**2b** (*S*,*S*,*S*,*R*)-NRB	
	#1 (79.1)	#2 (20.3)	#1 (82.6)	#2 (8.7)
ψ_1	−14.2	−46.5	−17.6	25.4
φ_1	−43.1	−56.6	−48.0	66.6
ψ_2	−57.7	−27.1	−14.2	31.2
φ_2	−43.3	−126.0	−35.9	−154.1
ψ_3	−20.2	18.4	−43.1	8.2
φ_3	−48.3	66.3	−47.3	58.8
ψ_4	−46.4	1.8	−26.5	14.3
φ_4	−121.1	−77.2	−144.5	−115.7

[a] Results for the two most populated clusters, covering above 90% of the total population, are reported. Populations (%) of the remaining 3 clusters are: 0.3, 0.3, and 0.0 for **2a**, 6.0, 1.9, 0.8 for **2b**. Geometries of the most representative structures of **2a** and **2b** are depicted in figures reported in the ESI, pp. S52 and S53, respectively.

Conclusions

We have prepared two model pentapeptides **2a** and **2b** containing the unnatural cysteine mimic, 3-benzylsulfanylnorbornene amino acid (NRB) in a short chain sequence of Ala/Aib. All the synthetic steps were optimized allowing the preparation of a satisfactory amount of the pentapeptides containing steric congested NRB in good yields with a new MW assisted protocol. The presence of the C5–C6 double bond in the norbornene scaffold opens the way to further functionalization and/or reduction directly on the model peptides. The conformation of the model compounds **2a** and **2b** was studied by both theoretical calculation and spectroscopic analyses and confirmed by X-ray analysis. Interestingly, all the collected data confirm that both NRB enantiomers possess a strong right-handed helicogenic effect in the presence of L-alanine, as previously observed for the unsubstituted norbornene AA, where this peculiar effect was explained by the network of weak hydrogen interactions stabilized by the rigid norbornane core.[16] Moreover crystal structure gave a proof of the stabilization mechanism of such core. These results open the way for the design and the synthesis of stable peptides able to modulate pharmacologically relevant PPIs.

Experimental

Synthetic procedures

Compounds **1** and **5** have been previously described.[10]

(1*S*,2*R*,3*R*,4*R*)-Ethyl 2-[(*S*)-2-aminopropanamido-3-(benzylthio)-bicyclo[2.2.1]heptane-2-carboxylate (6a) and (1*R*,2*S*,3*S*,4*S*)-ethyl 2-[(*S*)-2-aminopropanamido-3-(benzylthio)bicyclo[2.2.1] heptane-

2-carboxylate (6b). To a solution of **5** (518 mg, 1.7 mmol) in dry DCM (10 mL), BSA (138 mg, 6.8 mmol) was added and let to react over-night at room temperature under stirring. FmocAlaF (638.5 mg, 2.04 mmol) was added and then the reaction mixture was made to react at room temperature for 20 minutes. The reaction was monitored by Tlc (AcOEt : *n*-hexane, 1 : 2; detected by ninhydrin). At the end of the reaction, the solvent was evaporated at reduced pressure and the crude purified by flash chromatography (eluent AcOEt : *n*-hexane, 1 : 6 to 1 : 2) affording the Fmoc derivatives in mixture (white solid, 85% yield) which were directly subjected to deprotection. The mixture was dissolved in the minimum amount of DMF (3 mL) and piperidine (150 μL) was added. The mixture was stirred at room temperature until disappearance of the reactants (1 h, Tlc AcOEt : *n*-hexane, 1 : 2; detected by ninhydrin). The solvent was evaporated at reduced pressure and the crude purified by flash chromatography (eluent DCM : MeOH, 100 : 0 to 50 : 1) affording small amounts of compound **6a** and **6b** (yellow solid, 95% overall yield) in pure form together with a major amount of their mixture.

6a. Mp 351–352 °C, $\alpha_D^{MeOH} = -85.95$. ^{1}H-NMR δ (200 MHz, $CDCl_3$): 8.62 (1H, s), 7.35–7.21 (5H, m), 4.26–4.10 (2H, m), 3.91–3.74 (2H, br s), 3.66–3.56 (1H, m), 3.21–3.16 (2H, m), 2.30–2.15 (2H, s), 1.94–1.88 (1H, d, J = 11 Hz), 1.48–1.21 (11H, m); ^{13}C-NMR δ (50 MHz, $CDCl_3$): 175.21, 173.59, 137.84, 129.13, 128.81, 127.51, 62.29, 61.40, 56.35, 51.18, 44.25, 42.41, 37.98, 36.55, 23.59, 22.75, 21.69, 14.37. (+)ESI-MS (m/z): 377.1 $[M + H]^+$. Anal. calcd for $C_{20}H_{28}N_2O_3S$ (376.1): C, 63.80; H, 7.50; N, 7.44; found C, 63.30; H, 7.38; N, 7.20; IR (KBr): ν = 3296, 2964, 1737, 1669 cm^{-1}.

6b. Mp 273–276 °C, α_D^{MeOH} = +117.75 ^{1}H-NMR δ (200 MHz, $CDCl_3$): 8.60 (1H, s), 7.32–7.23 (5H, m), 4.24–4.16 (2H, m), 3.90–3.76 (2H, br s), 3.60–3.54 (1H, m), 3.21–3.17 (2H, m), 2.32 (1H, s), 1.92–1.87 (1H, d, J = 11 Hz), 1.65 (2H, s), 1.48–1.22 (11H, m); ^{13}C-NMR δ (50 MHz, $CDCl_3$): 175.61, 173.76, 137.93, 129.12, 128.76, 127.46, 62.32, 61.40, 56.45, 51.31, 44.21, 42.46, 38.03, 36.50, 23.47, 22.72, 22.09, 14.36. (+)ESI-MS (m/z): 377.1 $[M + H]^+$. Anal. calcd for $C_{20}H_{28}N_2O_3S$ (376.1): C, 63.80; H, 7.50; N, 7.44; found C, 64.15; H, 7.55; N, 7.18; IR (KBr): ν = 3298, 2963, 1733, 1668 cm^{-1}.

(1*R*,2*R*,3*R*,4*S*)-Ethyl 2-((*S*)-2-acetamidopropanamido)-3-(benzylthio)bicyclo[2.2.1]heptane-2-carboxylate (7a). Compound **6a** (102 mg, 0.270 mmol) was dissolved in dry DCM (5 mL) under nitrogen and TEA (56.48 μL, 0.406 mmol) and acetic anhydride (38.34 μL, 0.406 mmol) were added under stirring at room temperature. The mixture was made to react until disappearance of the reactants (2 h, Tlc DCM : MeOH, 10 : 1; detected by ninhydrin). The organic phase was washed with HCl (0.1 N), saturated $NaHCO_3$ and then was dried over Na_2SO_4 and the solvent evaporated at reduced pressure to afford the acetylated ester (yellow oil, 75% yield) which was directly submitted to ester hydrolysis. The crude (83 mg) was dissolved in DCM : MeOH (9 : 1, 2 mL) and a methanolic solution of NaOH (201 μL, 0.64 mmol) was added. The mixture was heated (50 °C) until disappearance of the reactants (12 h, Tlc DCM : MeOH, 10 : 1). The solvent was evaporated at reduced pressure and the crude extracted with diethyl ether. The aqueous phase was taken up and cooled to 0 °C before adding HCl 1 N to pH = 2. The acidic aqueous phase was extracted with cold AcOEt, the organic phase was dried over Na_2SO_4 and the solvent evaporated at reduced pressure to afford a mixture containing **6a** as the major compound together with the diastereisomeric compound containing the *R*-alanine.

7a. ^{1}H-NMR δ (200 MHz, CD_3OD): 8.14 (1H, s), 7.34–7.19 (5H, m), 4.53–4.43 (1H, m), 3.87–3.73 (2H, m), 3.16 (1H, s), 3.06 (1H, s), 2.21 (1H, s), 1.99 (3H, s), 1.92–1.87 (1H, m), 1.46–1.18 (8H, m). ^{13}C-NMR δ (50 MHz, CD_3OD): 176.88, 174.20, 173.79, 137.93, 129.17, 129.11, 127.86, 64.91, 51.35, 49.15, 46.09, 42.65, 36.95, 35.82, 22.93, 21.07, 16.23, 15.46. (+)ESI-MS (m/z): 377.3 $[M - COMe]^+$. Anal. calcd for $C_{20}H_{30}N_2O_4S$ (418.55): C, 63.13; H, 7.22; N, 6.69; found C, 63.40; H, 7.27; N, 6.30; IR (KBr): ν = 3435, 2850, 1721, 1638 cm^{-1}.

(*S*)-*tert*-Butyl(1-((1-amino-1-oxopropan-2-yl)amino)-2-methyl-1-oxopropan-2-yl)carbamate (10). To a solution of BocAibOH **8** in dry DCM (0.1 M), HOAt (1.1 eq.) and EDC (1.1 eq.) were added under nitrogen at 0 °C and let to react under stirring at 0 °C for 1 h. After that, l-AlaCONH$_2$ **9** (1.1 eq.) and DIPEA (2.2 eq.) were added, followed by DIPEA to reach pH = 8, and then the reaction mixture was made to react at room temperature for 12 h. The reaction was monitored by Tlc (MeOH : DCM, 1 : 10; detected by ninhydrin). Upon the consumption of the starting material the reaction mixture was washed with saturated NH_4Cl, saturated $NaHCO_3$, and brine. The organic phase was dried over Na_2SO_4 and the solvent evaporated at reduced pressure to afford compound **10** as white wax (75% yield). The reaction was performed with comparable yield from 0.1 g to 2 g. $\alpha_D^{MeOH} = -7.6$. ^{1}H-NMR δ (200 MHz, $CDCl_3$): 7.08 (1H, s), 6.53 (1H, d, J = 7.2 Hz), 5.34 (1H, s), 5.01 (1H, s), 4.54–4.39 (1H, m), 1.79–1.40 (18H, m); ^{13}C-NMR δ (50 MHz, $CDCl_3$) 175.04, 174.25, 155.47, 81.14, 57.02, 49.09, 28.46, 26.63, 24.75, 17.85. (+)ESI-MS (m/z): $[M + Na]^+$ 296.1. Anal. calcd for $C_{12}H_{23}N_3O_4$ (273.17): C, 52.73; H, 8.48; N, 15.37; found C, 52.78; H, 8.53; N, 15.40. IR (KBr): ν = 3400, 3370, 2984, 1693, 1673, 1515 cm^{-1}.

(*S*)-2-Amino-*N*-(1-amino-1-oxopropan-2-yl)-2-methylpropanamide (11). Trifluoroacetic acid 99% (TFA, 30 eq.) was added dropwise under stirring to a solution of compound **10** (1 eq.) in dry DCM (0.1 M) at 0 °C. The solution was warmed up at room temperature and let to react for 4 hours. The reaction was monitored by Tlc (MeOH : DCM, 1 : 10; detected by ninhydrin). Upon consumption of the starting material the solvent was evaporated at reduced pressure to afford the desired compound **11** as light yellow oil (92% yield). The reaction was performed with comparable yield from 0.1 g to 2 g. Mp 254 °C, α_D^{MeOH} = +4.28. ^{1}H-NMR δ (200 MHz, CD_3OD): 4.43–4.32 (1H, m), 1.59 (6H, d, J = 5.19 Hz), 1.41 (3H, d, J = 11.54 Hz); ^{13}C-NMR δ (50 MHz, CD_3OD): 175.98, 171.65, 57.01, 49.35, 22.94, 22.81, 16.85. (+)ESI-MS (m/z): $[M + Na]^+$ 174.1. Anal. calcd for $C_9H_{16}F_3N_3O_4$ (173.12 + 114): C, 37.63; H, 5.61; N, 14.63; found C, 37.68; H, 5.58; N, 14.67; IR (NaCl): ν = 3418, 2095, 1673, 1545, 1204 cm^{-1}.

***tert*-Butyl((*S*)-1-((1-(((*S*)-1-amino-1-oxopropan-2-yl)amino)-2-methyl-1-oxopropan-2-yl)amino)-1-oxopropan-2-yl)carbamate (13).** To a solution of Boc-(l)AlaOH **12** in dry DCM (0.1 M), HOAt (1.1 eq.) and EDC (1.1 eq.) were under nitrogen at 0 °C and let to

react under stirring at 0 °C for 1 h. After that, **11** (1.1 eq.) and DIPEA (2.2 eq.) were added, followed by additional DIPEA to reach pH = 8, and then the reaction mixture was made to react at room temperature for 12 h. The reaction was monitored by Tlc (MeOH : DCM, 1 : 10; R_f 0.19, detected by ninhydrin). Upon the consumption of the starting material the reaction mixture was washed with saturated NH_4Cl, saturated $NaHCO_3$, and brine. The saturated NH_4Cl solution of the first washing was re-extracted 3 times with EtOAc and the combined organic phases dried over Na_2SO_4. The solvent was evaporated at reduced pressure and the crude purified by flash chromatography (eluent MeOH : DCM, 1 : 10 to 1 : 5) to afford compound **13** as white wax (69% yield). The reaction was performed with comparable yield from 0.1 g to 2 g. $\alpha_D^{MeOH} = -20$. ^{1}H-NMR δ (200 MHz, CD_3OD): 4.21 (1H, q, $J = 7.3$ Hz), 3.88 (1H, q, $J = 7.3$ Hz), 1.60–1.39 (18H, m), 1.30 (3H, d, $J = 7.3$ Hz). ^{13}C-NMR δ (50 MHz, CD_3OD): 177.00, 175.50, 175.31, 157.18, 79.88, 56.54, 51.96, 49.76, 27.53, 25.34, 23.32, 16.53, 16.02. (+)ESI-MS (*m*/*z*): $[M + Na]^+$ 367.2. Anal. calcd for $C_{15}H_{28}N_4O_5$ (344.4): C, 52.31; H, 8.19; N, 16.27; found C, 52.36; H, 8.24; N, 16.31. IR (KBr): ν = 3410, 3310, 2981, 2938, 1679, 1665, 1536 cm^{-1}.

***N*-((*S*)-1-Amino-1-oxopropan-2-yl)-2-((*S*)-2-aminopropanamido)-2-methylpropanamide (4) (HAla-Aib-AlaNH$_2$).** Compound **13** was dissolved in water (0.1 M) in a sealed tube for microwaves reactor. The solution was irradiated by microwaves under magnetic stirring for 20 min at 150 °C. The reaction was monitored by Tlc (MeOH : DCM, 1 : 10; detected by ninhydrin). If not finished, another round of 20 minutes was performed. Upon consumption of the starting material, water was evaporated at reduced pressure to afford the desired compound **4** as light yellow solid (94% yield). The reaction was performed with comparable yield from 0.1 g to 2 g. $\alpha_D^{MeOH} = -1.55$. ^{1}H-NMR δ (200 MHz, CD_3OD): 4.30 (1H, q, J = 7.2 Hz), 3.44 (1H, q, $J = 6.9$ Hz), 1.46–1.26 (12H, m); ^{13}C-NMR δ (50 MHz, CD_3OD): 176.70, 176.67, 175.32, 56.32, 50.38, 49.28, 24.48, 23.86, 19.65, 16.54. (+)ESI-MS (*m*/*z*): $[M + Na]^+$ 244.15. Anal. calcd for $C_{10}H_{20}N_4O_3$ (267.3): C, 49.17; H, 8.25; N, 22.93; found C, 49.22; H, 8.29; N, 22.98. IR (KBr): $\nu = 3399$, 3064, 2985, 1660, 1530 cm^{-1}.

(1*R,2*R**,3*R**,4*S**)-Ethyl-3-(benzylthio)-2-((*tert*-butoxycarbonyl)-amino bicyclo[2.2.1]hept-5-ene-2-carboxylate (14).** To solution of compound **1** in dry DCM (0.1 M), Boc-anhydride (2 eq.) followed by dry TEA (2 eq.) were added at 0 °C and let to react at rt for 4 h. The reaction is monitored bt Tlc (EtOAc : hexane, 1 : 2; detected by ninhydrin). Upon the consumption of the starting material the crude mixture was diluted with DCM and washed with HCl 1 M, saturated $NaHCO_3$, and brine. The organic phase was dried over Na_2SO_4 and the solvent was evaporated at reduced pressure. The crude product was purified by flash chromatography (eluent EtOAc : hexane, from 1 : 6 to 1 : 2) affording **14** in pure form as colorless oil (90% yield). The reaction was performed with comparable yield from 0.1 g to 2 g.

^{1}H-NMR δ (200 MHz, $CDCl_3$): 7.30 (5H, bs), 6.19–6.10 (2H, m), 5.84 (1H, s), 4.26–4.19 (2H, m), 3.79 (2H, s), 3.65 (1H, s), 3.49 (1H, s), 2.89 (1H, s), 1.82 (1H, d, $J = 9.3$ Hz), 1.58–1.46 (10H, m), 1.29 (3H, t, $J = 7.1$ Hz). ^{13}C-NMR δ (50 MHz, $CDCl_3$): 174.06, 154.98, 138.01, 137.27, 136.69, 129.10, 128.77, 127.40, 79.69, 64.09, 61.56, 56.51, 50.41, 48.55, 47.39, 37.15, 28.55, 14.39. (+) ESI-MS (*m*/*z*): $[M + Na]^+$ 426.2. Anal. calcd for $C_{22}H_{29}NO_4S$ (403.3): C, 65.48; H, 7.24; N, 3.47; found C, 65.53; H, 7.20; N, 3.42; IR (KBr): $\nu = 3358$, 2979, 1738, 1714, 1530 cm^{-1}.

(1*R,2*R**,3*R**,4*S**)-3-(Benzylthio)-2-((*tert*-butoxycarbonyl)-amino)bicyclo[2.2.1]hept-5-ene-2-carboxylic acid (15).** To solution of compound **14** in dry DCM : MeOH (9 : 1, 0.1 M) in a sealed reactor, a solution of KOH in MeOH 6 M (20 eq.) was added and let to react at 70 °C for 8 h. The reaction is monitored bt Tlc (EtOAc : hexane, 1 : 2; detected by ninhydrin and UV light). Upon the consumption of starting material the reaction mixture was filtered, the organic solvent was evaporated and the crude was dissolved in HCl 1 M at 0 °C until pH = 2. Then it was extracted 3 times in EtOAc. The combined organic phases was dried over Na_2SO_4 and the solvent was evaporated at reduced pressure affording **15** in pure form as colorless wax (88% yield). The reaction was performed with comparable yield from 0.1 g to 1.0 g. ^{1}H-NMR δ (200 MHz, $CDCl_3$): 7.37–7.23 (5H, m), 6.25–6.20 (1H, m), 6.14 (1H, s), 6.02–6.00 (1H, m), 4.16 (1H, d, $J = 3.1$ Hz), 3.74 (1H, s), 3.67 (2H, s), 3.02 (1H, s), 1.69 (1H, d, $J = 9.6$ Hz), 1.54 (1H, d, $J = 9.8$ Hz), 1.47 (9H, s). ^{13}C-NMR δ (50 MHz, $CDCl_3$): 174.61, 158.59, 138.01, 137.26, 135.74, 129.12, 128.89, 127.51, 82.04, 65.05, 55.68, 50.25, 48.82, 46.05, 37.75, 28.46. (+) ESI-MS (*m*/*z*): $[M + Na]^+$ 398.2. Anal. calcd for $C_{20}H_{25}NO_4S$ (375.15): C, 63.97; H, 6.71; N, 3.73; found C, 63.92; H, 6.65; N, 3.77; IR (KBr): $\nu = 3339$, 2965, 1715, 1485, 1394 cm^{-1}.

***tert*-Butyl((1*R*,2*R*,3*R*,4*S*)-2-(((*S*)-1-((1-(((*S*)-1-amino-1-oxopropan-2-yl)amino)-2-methyl-1-oxopropan-2-yl)amino)-1-oxopropan-2-yl)-carbamoyl)-3-(benzylthio)bicyclo[2.2.1]hept-5-en-2-yl)carbamate-(16a)**

*tert-Butyl((1S,2S,3S,4R)-2-(((S)-1-((1-(((S)-1-amino-1-oxopropan-2-yl)amino)-2-methyl-1-oxopropan-2-yl)amino)-1-oxopropan-2-yl)-carbamoyl)-3-(benzylthio)bicyclo[2.2.1]hept-5-en-2-yl)carbamate (**16b**).* To a solution of **15** in dry DCM (0.1 M), HOAt (1.1 eq.) and EDC (1.1 eq.) were added under nitrogen at 0 °C and let to react under stirring at 0 °C for 1 h. After that, **4** (HAla-Aib-AlaNH$_2$) (1.1 eq.) and DIPEA (2.2 eq.) were added, followed by additional DIPEA to reach pH = 8 and the reaction mixture was made to react at room temperature for 8 h. The reaction was monitored by Tlc (MeOH : DCM, 1 : 10; detected by ninhydrin or UV light). Upon the consumption of the starting material the reaction mixture was washed with saturated NH_4Cl, saturated $NaHCO_3$, and brine. The NH_4Cl saturated solution was extracted 3 times with EtOAc. The combined organic phases were dried over Na_2SO_4 and the solvent evaporated at reduced pressure. The crude was purified by flash chromatography (GraceResolv silica cartridges, eluent DCM : MeOH, 120 : 1 to 10 : 1) affording pure compounds **16a** and **16b**. The reaction was performed with comparable yield from 0.1 g to 1 g.

16a (white solid, Mp = 101 °C); yield: 37%. $\alpha_D^{MeOH} = +50$. ^{1}H-NMR δ (200 MHz, $CDCl_3$): 7.57–7.55 (2H, m), 7.39–7.23 (6H, m), 6.72 (1H, d, $J = 2.5$ Hz), 6.32 (1H, dd, $J = 5.5$, 2.9 Hz), 6.07 (1H, dd, $J = 5.5$, 3.1 Hz), 5.94 (1H, s), 5.86 (1H, s), 4.43 (1H, dq, $J = 7.7$, 7.9 Hz), 3.93 (1H, qd, $J = 7.2$, 3.9 Hz), 3.70 (2H, s), 3.62 (1H, s), 3.39 (1H, d, $J = 3.0$ Hz), 3.01 (1H, s), 2.18 (1H, d, $J = 9.3$ Hz), 1.64–1.51 (6H, m), 1.51–1.44 (12H, m), 1.44–1.34 (4H, m); ^{13}C-NMR δ (50 MHz, $CDCl_3$): 175.73, 174.31, 173.44, 173.35, 156.61, 137.74, 137.35, 137.27, 129.10, 128.74, 127.96, 81.70, 64.54, 57.45, 56.93, 52.57, 51.13, 49.66, 48.72, 47.38, 37.86,

28.42, 27.83, 23.69, 17.46, 17.28. (+)ESI-MS (m/z): $[M + Na]^+$ 624.4. Anal. calcd for $C_{30}H_{43}N_5O_6S$ (601.3): C, 59.88; H, 7.20; N, 11.64; found C, 59.96; H, 7.23; N, 11.61. IR (KBr): $\nu = 3327, 2981, 1660, 1531, 1455\ cm^{-1}$.

16b (white solid, Mp = 134 °C); yield 37%. $\alpha_D^{MeOH} = -66.1$. ^{1}H-NMR δ (200 MHz, $CDCl_3$): 7.96 (1H, s), 7.43 (1H, d, $J = 7.44$ Hz), 7.27–7.26 (5H, m), 6.75 (1H, d, $J = 3.6$ Hz), 6.58–6.54 (1H, m), 6.28–6.24 (1H, m), 5.29 (1H, s), 4.88 (1H, s), 4.33 (1H, t, $J = 7.3$ Hz), 4.24 (1H, d, $J = 3.6$ Hz), 4.06–4.01 (1H, m), 3.60 (2H, s), 3.06 (1H, s), 3.03 (1H, s), 1.75 (1H, d, $J = 9.5$ Hz), 1.62–1.34 (22H, m). ^{13}C-NMR δ (50 MHz, $CDCl_3$): 176.38, 174.59, 173.81, 173.30, 157.38, 142.78, 138.37, 133.19, 128.77, 128.66, 127.42, 81.70, 70.50, 57.52, 54.27, 53.53, 52.67, 50.06, 49.96, 45.88, 39.25, 28.42, 27.71, 23.96, 17.72, 17.42. (+)ESI-MS (m/z): $[M + Na]^+$ 624.4. Anal. calcd for $C_{30}H_{43}N_5O_6S$ (601.3): C, 59.88; H, 7.20; N, 11.64; found C, 59.92; H, 7.25; N, 11.60. IR (KBr): $\nu = 3310, 2981, 1657, 1532\ cm^{-1}$.

(1*R*,2*R*,3*R*,4*S*)-2-Amino-*N*-((*S*)-1-((1-(((*S*)-1-amino-1-oxopropan-2-yl)amino)-2-methyl-1-oxopropan-2-yl)amino)-1-oxopropan-2-yl)-3-(benzylthio)bicyclo[2.2.1]hept-5-ene-2-carboxamide (17a). Compound **16a** was dissolved in water (0.1 M) in a sealed tube for microwaves reactor. The solution was irradiated by microwaves under magnetic stirring for 30 min at 150 °C. The reaction was monitored by Tlc (MeOH : DCM, 1 : 10; detected by ninhydrin). If not finished, another round of 20 minutes was performed. Upon consumption of the starting material water was evaporated at reduced pressure. The crude was purified by flash chromatography (GraceResolv silica cartridges; eluent MeOH : DCM, 1 : 20 to 1 : 1) to afford compound **17a** in a pure form as white solid (88% yield). The reaction was performed with comparable yield from 0.1 g to 0.4 g. Mp 65 °C; $\alpha_D^{MeOH} = +38.57$. ^{1}H-NMR δ (200 MHz, $CDCl_3$): 7.77 (1H, d, $J = 3.6$ Hz), 7.33–7.16 (7H, m), 6.52 (1H, s), 6.42 (1H, dd, $J = 5.6$, 3.0 Hz), 6.19 (1H, dd, $J = 5.6$, 3.0 Hz), 5.40 (1H, s), 4.42–4.35 (1H, m), 4.00 (1H, d, $J = 3.4$ Hz), 3.97–3.84 (1H, m), 3.69 (1H, d, $J = 13.6$ Hz, AB system), 3.64 (1H, d, $J = 13.7$ Hz, AB system), 3.11 (1H, s), 2.77 (1H, s), 2.04 (1H, d, $J = 8.8$ Hz), 1.53–1.34 (15H, m); ^{13}C-NMR δ (50 MHz, $CDCl_3$): 178.48, 175.69, 173.56, 173.03, 140.10, 139.48, 134.94, 128.96, 128.86, 127.35, 66.77, 56.96, 55.61, 54.81, 51.44, 49.87, 49.73, 45.72, 38.57, 27.49, 23.93, 17.54, 16.52. (+)ESI-MS (m/z): $[M + Na]^+$ 524.4. Anal. calcd for $C_{25}H_{35}N_5O_4S$ (501.3): C, 59.86; H, 7.03; N, 13.96; found C, 59.82; H, 7.09; N, 13.91; IR (KBr): $\nu = 3310, 2980, 1657, 1522\ cm^{-1}$.

(1*R*,2*S*,3*S*,4*S*)-2-Amino-*N*-((*S*)-1-((1-(((*S*)-1-amino-1-oxopropan-2-yl)amino)-2-methyl-1-oxopropan-2-yl)amino)-1-oxopropan-2-yl)-3-(benzylthio)bicyclo[2.2.1]heptane-2-carboxamide (17b). Compound **16b** was dissolved in water (0.1 M) in a sealed tube for microwaves reactor. The solution was irradiated by microwaves under magnetic stirring for 30 min at 150 °C. The reaction was monitored by Tlc (MeOH : DCM, 1 : 10; detected by ninhydrin). If not finished, another round of 20 minutes was performed. Upon consumption of the starting material water was evaporated at reduced pressure. The crude of reaction was purified by chromatography (GraceResolv silica cartridges, eluent MeOH : DCM, 1 : 20 to 1 : 15) to afford compound **17b** in a pure form as colorless wax (82% yield). The reaction was performed with comparable yield from 0.1 g to 0.4 g, $\alpha_D^{MeOH} = -7.65$. ^{1}H-NMR δ (200 MHz, $CDCl_3$): 8.10 (1H, d, $J = 4.6$ Hz), 7.36–7.20 (5H, m), 7.10 (1H, d, $J = 7.7$ Hz), 7.02 (1H, s), 6.71 (1H, s), 6.43 (1H, dd, $J = 5.5$, 2.9 Hz), 6.24 (1H, dd, $J = 5.6$, 3.0 Hz), 5.49 (1H, s), 4.46–4.23 (1H, m), 4.12 (1H, dt, $J = 12.0$, 7.1 Hz), 3.92 (1H, d, J 3.3 Hz), 3.70 (2H, s), 3.01 (1H, s), 2.95 (1H, s), 2.00 (1H, d, $J = 9.5$ Hz), 1.67–1.25 (15H, m); ^{13}C-NMR δ (50 MHz, $CDCl_3$): 178.14, 175.44, 173.72, 172.79, 140.13, 138.2, 134.98, 128.91, 128.79, 127.55, 66.53, 57.15, 55.01, 54.31, 51.45, 49.71, 48.58, 46.25, 37.38, 26.78, 24.58, 17.50, 16.9. (+)ESI-MS (m/z): $[M + Na]^+$ 524.4. Anal. calcd for $C_{25}H_{35}N_5O_4S$ (501.3): C, 59.86; H, 7.03; N, 13.96; found C, 59.89; H, 7.09; N, 13.89. IR (KBr): $\nu = 3317, 2975, 1653, 1521\ cm^{-1}$.

(1*R*,2*R*,3*R*,4*S*)-2-((*S*)-2-Acetamidopropanamido)-*N*-((*S*)-1-((1-(((*S*)-1-amino-1-oxopropan-2-yl)amino)-2-methyl-1-oxopropan-2-yl)amino)-1-oxopropan-2-yl)-3-(benzylthio)bicyclo[2.2.1]hept-5-ene-2-carboxamide (2a). (l)Ac-Ala-OH (1 eq.) was dissolved in dry DCM (0.1 M) and HOAt (1.1 eq.) and EDC (1.1 eq.) were added under nitrogen at 0 °C. The mixture was made to react under stirring at 0 °C for 1 h. After that, **17a** (NRB-Ala-Aib-AlaCONH$_2$) (1.1 eq.) and DIPEA (2.2 eq.) were added followed by additional DIPEA to reach pH = 8, and then the reaction mixture was let to react at room temperature for 12 h. The reaction was monitored by HPTlc (MeOH : DCM, 1 : 10; detected by ninhydrin or UV light and checked by ^{1}H-NMR). Upon the consumption of the starting material the reaction mixture was washed with saturated NH_4Cl, saturated $NaHCO_3$, and brine. The NH_4Cl, saturated solution was extracted 3 times with EtOAc. The combined organic phases were dried over Na_2SO_4 and the solvent evaporated at reduced pressure. The crude was purified by inverse phase HPLC (eluent 95% H_2O, 5% CH_3CN, 0.1% TFA to 70% H_2O 30% CH_3CN 0.1% TFA) to afford pure compound **2a** as solid wax (40% yield). Recovered starting material (40%). The reaction was performed with comparable yield from 0.1 g to 2 g. $\alpha_D^{MeOH} = 146.4$. ^{1}H-NMR δ (500 MHz, CD_3CN): 7.96 (1H, bs), 7.85 (1H, s), 7.65 (1H, bs), 7.41–7.28 (7H, m), 7.10 (1H, s), 6.28 (1H, dd, $J = 5.6$, 2.8 Hz), 6.19 (1H, bs), 6.09 (1H, s), 4.19–3.94 (1H, m), 4.15–4.07 (1H, m), 4.05–4.00 (1H, m), 3.83 (1H, d, $J = 13.5$ Hz, AB system), 3.66 (1H, d, $J = 13.5$ Hz, AB system), 3.64 (1H, s), 3.36 (1H, s), 2.90 (1H, s), 2.20 (1H, d, $J = 8.2$ Hz), 2.04 (3H, s), 1.51 (3H, s), 1.50 (3H, s), 1.48–1.45 (4H, m), 1.39 (3H, d, $J = 3.9$ Hz), 1.37 (3H, d, $J = 3.9$ Hz); ^{13}C-NMR δ (126 MHz, CD_3CN): 176.42, 175.37, 174.63, 174.59, 173.32, 173.13, 137.81, 137.35, 136.48, 131.26, 128.77, 127.46, 67.76, 56.68, 56.43, 52.39, 52.26, 50.48, 49.70, 48.39, 47.16, 36.32, 26.61, 22.70, 21.92, 16.54, 16.03, 15.80. (+)ESI-MS (m/z): $[M + Na]^+$ 637.4. Anal. calcd for $C_{30}H_{42}N_6O_6S$ (614.3): C, 58.61; H, 6.89; N, 13.67; found C, 58.62; H, 6.89; N, 13.68. IR (KBr): $\nu = 3333, 2974, 1656, 1529\ cm^{-1}$.

(1*S*,2*S*,3*S*,4*R*)-2-((*S*)-2-Acetamidopropanamido)-*N*-((*S*)-1-((1-(((*S*)-1-amino-1-oxopropan-2-yl)amino)-2-methyl-1-oxopropan-2-yl)amino)-1-oxopropan-2-yl)-3-(benzylthio)bicyclo[2.2.1]hept-5-ene-2-carboxamide (2b). In a sealed tube for microwaves reactor, compound **17b** was dissolved in THF (0.1 M) and EEDQ (1.1 eq.) and (l)-Ac-Ala-OH (1 eq.) were added. The solution was irradiated by microwave under magnetic stirring for 30 min at 60 °C (power: 80 Watt) using the air compressing cooling system of the reactor to keep down the temperature. The reaction was

monitored by HPTlC (5 × 7.5 cm silica gel 60 F_{254}, MERCK) (MeOH : DCM, 1 : 10; detected by ninhydrin). If not finished another round of 30 minutes was performed. Upon consumption of the starting material the tube was cooled down in an ice bath and the precipitate was filtered affording pure compound **2b** as white solid (Mp: 76 °C) without the need of further purification (yield: 60%). The slow precipitation in a concentrated solution of compound **2b** in CH_3CN permitted the obtainment of a single crystal for X-ray analysis. The reaction was performed with comparable yield from 50 mg to 100 mg, $\alpha_D^{MeOH} = -89.6$. ^{1}H-NMR δ (500 MHz, CD_3CN): 7.73 (1H, s), 7.52 (1H, d, $J = 4.8$ Hz), 7.35–7.31 (5H, m), 7.29–7.24 (1H, m), 7.08 (1H, s), 7.02 (1H, s), 6.95 (1H, d, $J = 5.8$ Hz), 6.41 (1H, dd, $J = 5.6$, 2.9 Hz), 6.29 (1H, dd, $J = 5.7$, 2.9 Hz), 5.58 (1H, s), 4.28 (1H, dq, $J = 5.8$, 7.15 Hz), 4.16 (1H, d, $J = 3.5$ Hz), 4.07 (1H, dq, $J = 7.36$, 7.36 Hz), 3.99 (1H, dq, $J = 4.8$, 7.3 Hz), 3.81 (1H, d, $J = 12.6$ Hz, AB system), 3.77 (1H, d, $J = 12.6$ Hz, AB system), 3.33 (1H, s), 3.04 (1H, s), 1.95 (3H, s), 1.80 (1H, d, $J = 9.3$ Hz), 1.49 (6H, d, $J = 1.3$ Hz), 1.45–1.38 (4H, m), 1.34 (3H, d, $J = 5.0$ Hz), 1.33 (3H, d, $J = 5.2$ Hz); ^{13}C-NMR δ (126 MHz, CD_3CN): 175.46, 174.49, 174.16, 173.93, 173.90, 171.45, 139.75, 138.60, 134.81, 128.78, 128.47, 126.96, 68.17, 56.60, 55.06, 52.40, 51.99, 50.31, 49.67, 49.08, 45.45, 38.10, 26.26, 23.19, 21.93, 16.95, 16.11, 15.83. (+)ESI-MS (m/z): $[M + Na]^+$ 637.4. Anal. calcd for $C_{30}H_{42}N_6O_6S$ (614.3): C, 58.61; H, 6.89; N, 13.67; found C, 58.66; H, 6.93; N, 13.64. IR (KBr): $\nu = 3310$, 2984, 1656, 1533 cm^{-1}.

Acknowledgements

This work was partially supported by Ministero dell'Università e della Ricerca (Prin 2010 "Synthesis and biomedical applications of tumor-targeting peptidomimetics" prot. 2010NRREPL. We also acknowledge the CINECA and the Regione Lombardia award under the LISA initiative, for the availability of high performance computing resources and support.

References

1 A. Mullard, *Nat. Rev. Drug Discovery*, 2012, **11**, 173–175.
2 R. J. Bienstock, *Curr. Pharm. Des.*, 2012, **18**, 1240–1254.
3 M. Rubinstein and M. Y. Niv, *Biopolymers*, 2009, **91**, 505–513; V. M. Ahrens, K. Bellmann-Sickert and A. G. Beck-Sickinger, *Future Med. Chem.*, 2012, **4**, 1567–1586.
4 L. Diao and B. Meibohm, *Clin. Pharmacokinet.*, 2013, **52**, 855–868.
5 (*a*) I. L. Karle and P. Balaram, *Biochemistry*, 1990, **29**, 6747–6756; (*b*) C. Toniolo, M. Crisma, F. Formaggio and C. Peggion, *Biopolymers*, 2001, **60**, 396–419; (*c*) M. C. Venkatachalam, *Biopolymers*, 1968, **6**, 1425–1436; (*d*) C. Toniolo, *Crit. Rev. Biochem.*, 1980, **9**, 1–44; (*e*) G. D. Rose, L. M. Gierasch and J. A. Smith, *Adv. Protein Chem.*, 1985, **37**, 1–109; (*f*) G. Némethy and M. P. Printz, *Macromolecules*, 1972, **5**, 755–758; (*g*) B. W. Matthews, *Macromolecules*, 1972, **5**, 818–819; (*h*) C. Toniolo and E. Benedetti, *Trends Biochem. Sci.*, 1991, **16**, 350–353; (*i*) C. Toniolo, M. Crisma, F. Formaggio, C. Peggion, Q. B. Broxterman and B. Kaptein, *Biopolymers*, 2004, **76**, 162–176.
6 (*a*) L. Gentilucci, D. R. Marco and L. Cerisoli, *Curr. Pharm. Des.*, 2010, **16**, 3185–3203; (*b*) S. Pellegrino, A. Contini, F. Clerici, A. Gori, D. Nava and M. L. Gelmi, *Chem.–Eur. J.*, 2012, **18**, 8705; (*c*) S. Pellegrino, A. Contini, M. L. Gelmi, L. Lo Presti, R. Soave and E. Erba, *J. Org. Chem.*, 2014, **79**, 3094.
7 E. Longo, A. Moretto, F. Formaggio and C. Toniolo, *Chirality*, 2011, **23**, 756–760.
8 F. Caputo, F. Clerici, M. L. Gelmi, S. Pellegrino and D. Pocar, *Tetrahedron: Asymmetry*, 2006, **17**, 1430–1436.
9 S. Pellegrino, F. Clerici and M. L. Gelmi, *Tetrahedron*, 2008, **64**, 5657–5665.
10 A. Ruffian, A. Casoni, S. Pellegrino, M. L. Gelmi, R. Soave and F. Clerici, *Tetrahedron*, 2012, **68**, 1951–1962.
11 M. L. Gelmi, C. Cattaneo, S. Pellegrino, F. Clerici, M. Montali and C. Martini, *J. Org. Chem.*, 2007, **72**, 9811–9814.
12 (*a*) M. A. Sussman, S. Welch, A. Walker, R. Klevitsky, T. E. Hewett, R. L. Price, E. Schaefer and K. Yager, *J. Clin. Invest.*, 2000, **105**, 875–886; (*b*) M. Satoh, H. Ogita, K. Takeshita, Y. Mukai, D. J. Kwiatkowski and J. K. Liao, *Proc. Natl. Acad. Sci. U. S. A.*, 2006, **103**, 7432–7437.
13 A. Ruffian, N. Ferri, S. K. Bernini, C. Ricci, A. Corsini, I. Maffucci, F. Clerici and A. Contini, *J. Med. Chem.*, 2014, **57**, 2953–2962.
14 (*a*) N. Ferri, S. K. Bernini, A. Corsini, F. Clerici, E. Erba, S. Stragliotto and A. Contini, *Med. Chem. Commun.*, 2013, **4**, 537–541; (*b*) N. Ferri, A. Corsini, P. Bottino, F. Clerici and A. Contini, *J. Med. Chem.*, 2009, **52**, 4087–4090.
15 A. Contini, unpublished results. On the Rac1 side, interactions with Tiam1 are mediated by two loops, switch 1 (AAs 25–39) and switch 2 (AAs 57–75), and by non-conserved residues between switches, ensuring proper GEF/Rac1 pairing. (Worthylake, D. K.; Rossman, K. L.; Sondek, J., *Nature*, 2000, **408**, 682.) Preliminary results from our laboratory show hot and warm spots in the 13 residue long helix of Tiam1, CR3 (I1187-L1199); however, this portion cannot be used as a standalone peptide inhibitor, since is predicted to be disordered. However, we observed trough preliminary calculations that non-natural helical peptides mimicking the Tiam1 CR3 sequence could maintain the ability to bind Rac1, without altering the conformation of switch 1 and 2.
16 I. Maffucci, S. Pellegrino, J. Clayden and A. Contini, *J. Phys. Chem. B*, 2015, **119**, 1350–1361.
17 A. Carpino, D. Sadat-Aalaee, H. G. Chao and R. H. De Selms, *J. Am. Chem. Soc.*, 1990, **112**, 9651–9652.
18 A. Thaqi, A. McCluskey and J. L. Scott, *Tetrahedron Lett.*, 2008, **49**, 6962–6964.
19 A. Mahindra, K. Nooney, S. Uraon, K. K. Sharma and R. Jain, *RCS Adv.*, 2013, **3**, 16810–16816.
20 V. Santagada, F. Fiorino, E. Perissutti, B. Severino, V. De Filippis, B. Vivenzio and G. Caliendo, *Tetrahedron Lett.*, 2001, **42**, 5171–5173.
21 C. Toniolo, E. Valente, F. Formaggio, M. Crisma, G. Pilloni, C. Corvaja, A. Toffoletti, G. V. Martinez, M. P. Hanson,

G. L. Millhauser, C. George and J. L. Flippen-Anderson, *J. Pept. Sci.*, 1995, **1**, 45–57.
22 G. R. Desiraju, *Chem. Commun.*, 2005, **28**, 2995–3001.
23 E. Borsini, G. Broggini, A. Contini and G. Zecchi, *Eur. J. Org. Chem.*, 2008, 2808–2816.
24 A. Contini, D. Nava and P. Trimarco, *J. Org. Chem.*, 2006, **71**, 159–166.
25 A. Contini, S. Leone, S. Menichetti, C. Viglianisi and P. Trimarco, *J. Org. Chem.*, 2006, **71**, 5507–5514.
26 L. Lo Presti, R. Soave and R. Destro, *J. Phys. Chem. B*, 2006, **110**, 6405–6414.
27 M. C. Aversa, C. Barattucci, P. Bonaccorsi and A. Contini, *J. Phys. Org. Chem.*, 2009, **22**, 1048–1057.
28 A. Contini and E. Erba, *RSC Adv.*, 2012, **2**, 10652–10660.
29 K. Wuthrich, in *NMR of Proteins and Nucleic Acids*, Wiley, NewYork, NY, 1986.
30 G. Jung, H. Bruckner, R. Bosch, V. Winter, H. Schaal and J. Strahle, *Liebigs Ann. Chem.*, 1983, **7**, 1096–1106.
31 T. A. Darden D. A. Case, T. E. Cheatham III, C. L. Simmerling, J. Wang, R. E. Duke, R. Luo, R. C. Walker, W. Zhang, K. M. Merz, B. Roberts, S. Hayik, A. Roitberg, G. Seabra, J. Swails, A. W. Goetz, I. Kolossváry, K. F. Wong, F. Paesani, J. Vanicek, R. M. Wolf, J. Liu, X. Wu, S. R. Brozell, T. Steinbrecher, H. Gohlke, Q. Cai, X. Ye, J. Wang, M.-J. Hsieh, G. Cui, D. R. Roe, D. H. Mathews, M. G. Seetin, R. Salomon-Ferrer, C. Sagui, V. Babin, T. Luchko, S. Gusarov, A. Kovalenko and P. A. Kollman, *AMBER 12*, 2012.
32 Y. Sugita and Y. Okamoto, *Chem. Phys. Lett.*, 1999, **314**, 141–151.
33 R. P. Joosten, T. A. H. te Beek, E. Krieger, M. L. Hekkelman, R. W. W. Hooft, R. Schneider, C. Sander and G. Vriend, *Nucleic Acids Res.*, 2011, **39**, D411–D419.